

SUPPLEMENTAL MATERIAL

Hulsmans et al., <https://doi.org/10.1084/jem.20171274>

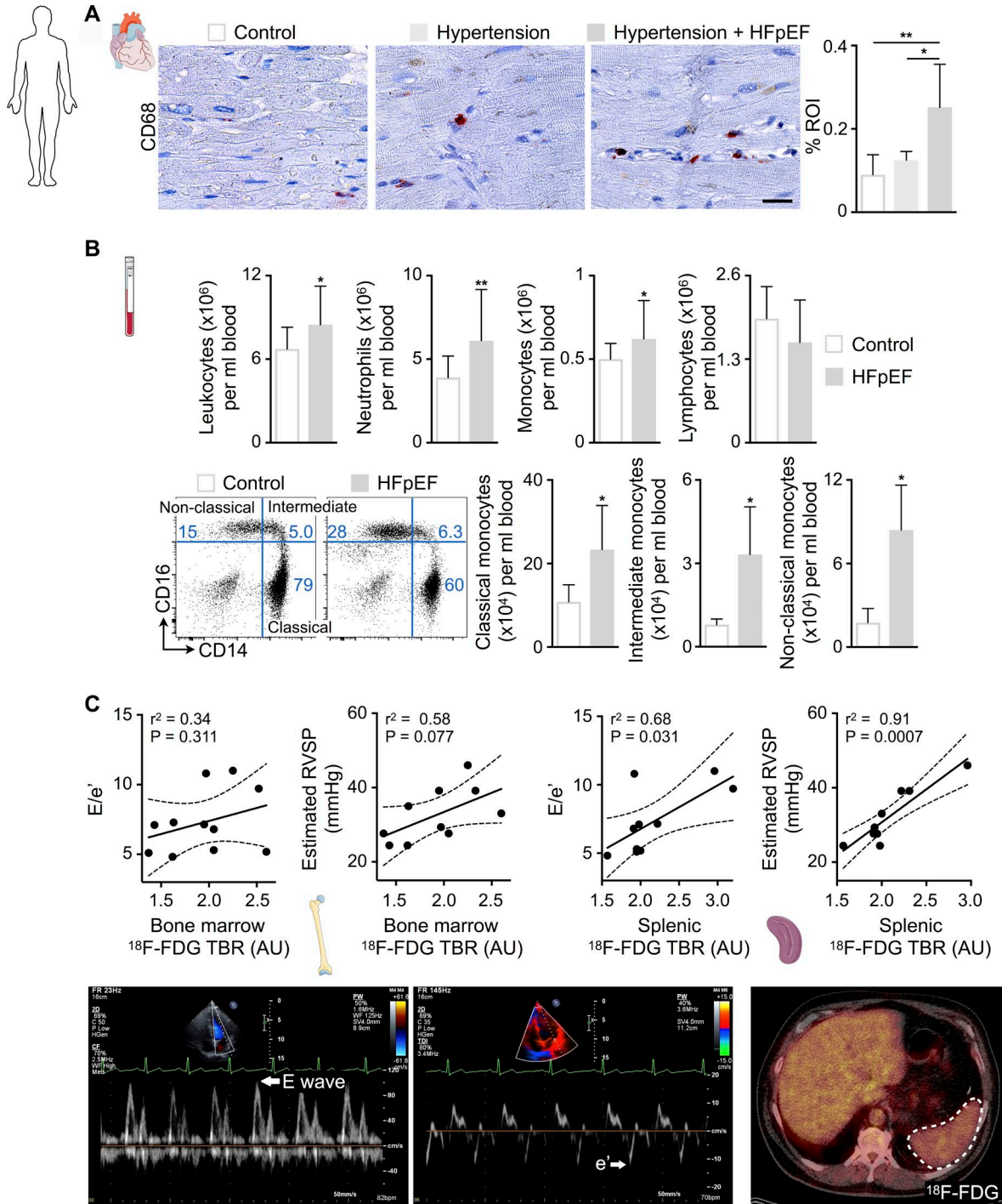


Figure S1. **Human data.** (A) Immunohistochemical stain for CD68 in LV myocardial biopsies from controls and hypertensive patients with and without HFpEF ($n = 4-6$ subjects per group). Left: Representative images; right: bar graph shows percentage of positive staining per ROI. Bar, 25 μm . (B) Top: Number of leukocytes, neutrophils, monocytes, and lymphocytes in blood from controls ($n = 10$) and HFpEF patients ($n = 20$); bottom: flow cytometric quantification of monocyte subsets in blood from controls ($n = 3$) and HFpEF patients ($n = 6$). (C) Top: Correlation between bone marrow or splenic ^{18}F -FDG uptake and echocardiographic parameters of diastolic function in healthy human subjects. Dashed lines indicate 95% confidence intervals of linear regression fit. AU, arbitrary units; r^2 , Pearson correlation coefficient; RVSP, right ventricular systolic pressure. Bottom: Representative echocardiographic and PET/CT images showing diastolic function assessment and ^{18}F -FDG uptake in human spleen, respectively. The dashed area indicates the spleen. Results are shown as mean \pm SD. For statistical analysis, a two-tailed unpaired t test was performed to compare two groups, and one-way ANOVA followed by Tukey's test was performed for multiple comparisons. *, $P < 0.05$; **, $P < 0.01$.

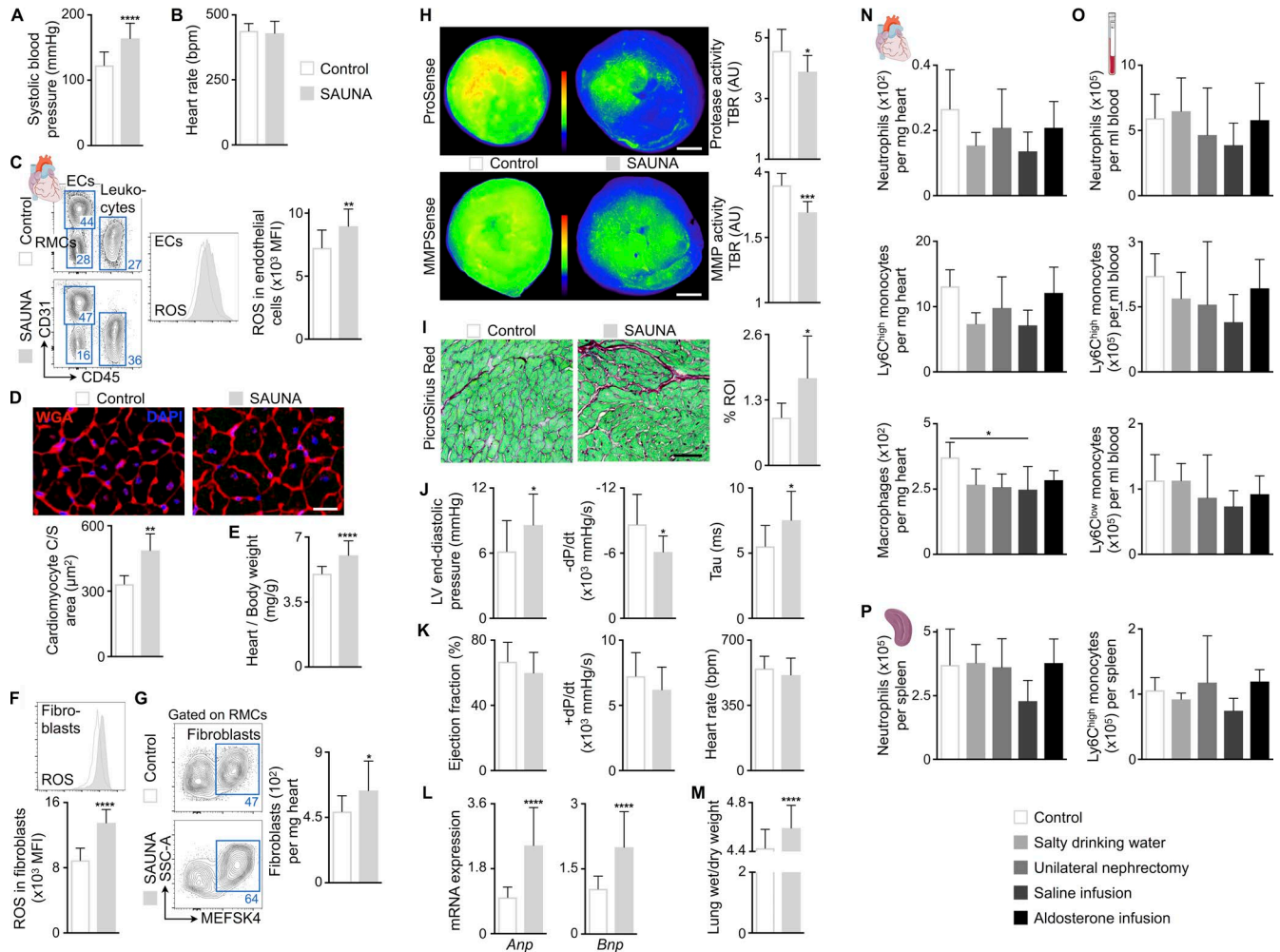


Figure S2. Cardiac phenotype in mice exposed to SAUNA. (A) Systolic blood pressure in control and SAUNA-exposed mice. Data are pooled from 10 independent experiments ($n = 44-74$ mice per group). (B) Heart rate in control and SAUNA-exposed mice by surface electrocardiogram. Data are pooled from two independent experiments ($n = 17-18$ mice per group). (C) Flow cytometric quantification of ROS production in cardiac endothelial cells (ECs) from control and SAUNA-exposed mice. Left: Representative flow cytometry plots; right: bar graph shows MFI indicating ROS production. Data are pooled from two independent experiments ($n = 11-14$ mice per group). The full gating strategy is shown in Fig. 7 D. (D) Top: Representative immunofluorescence images of control and SAUNA heart tissue stained with WGA (red) and DAPI (blue); bottom: bar graph shows cardiomyocyte cross-sectional (C/S) area in control and SAUNA hearts. Data are pooled from two independent experiments ($n = 6$ mice per group). Bar, 20 μm . (E) Heart-to-body weight ratio in control and SAUNA-exposed mice. Data are pooled from 20 independent experiments ($n = 121-134$ mice per group). (F) Flow cytometric quantification of ROS production in cardiac fibroblasts from control and SAUNA-exposed mice. Top: Representative flow cytometry plot; bottom: bar graph shows MFI indicating ROS production. Data are pooled from two independent experiments ($n = 11-14$ mice per group). (G) Flow cytometric quantification of fibroblasts in hearts from control and SAUNA-exposed mice. Left: Representative flow cytometry plots; right: bar graph shows number of fibroblasts per milligram of heart tissue. Data are pooled from two independent experiments ($n = 15-16$ mice per group). The full gating strategy is shown in Fig. 7 D. (H) Quantification of protease and MMP activity by fluorescence reflectance imaging in hearts from control and SAUNA-exposed mice. Data are pooled from two independent experiments ($n = 8-10$ mice per group). Bars, 1 mm. (I) Histological analysis of collagen deposition (PicroSirius Red) in hearts from control and SAUNA-exposed mice. Left: Representative images; right: bar graph shows percentage of positive staining per ROI. Data are pooled from two independent experiments ($n = 6$ mice per group). Bar, 50 μm . (J) Diastolic and (K) systolic parameters by pressure-volume catheterization of hearts from control and SAUNA-exposed mice. Data are pooled from two independent experiments ($n = 10-15$ mice per group). (L) Relative *Anp* and *Bnp* expression levels by qPCR in hearts from control and SAUNA-exposed mice. Data are pooled from seven independent experiments ($n = 50-52$ mice per group). (M) Lung wet-to-dry weight ratio in control and SAUNA-exposed mice. Data are pooled from eight independent experiments ($n = 52-64$ mice per group). (N-P) Flow cytometric quantification of myeloid cells in hearts (N), blood (O), and spleens (P) from untreated mice (control) and mice exposed to salty drinking water, unilateral nephrectomy, saline, or aldosterone infusion for 30 d. Data are pooled from two independent experiments ($n = 5$ mice per group). Results are shown as mean \pm SD. For statistical analysis, a two-tailed unpaired *t* test was performed to compare two groups, and one-way ANOVA followed by Tukey's test was performed for multiple comparisons. *, $P < 0.05$; **, $P < 0.01$; ***, $P < 0.001$; ****, $P < 0.0001$.

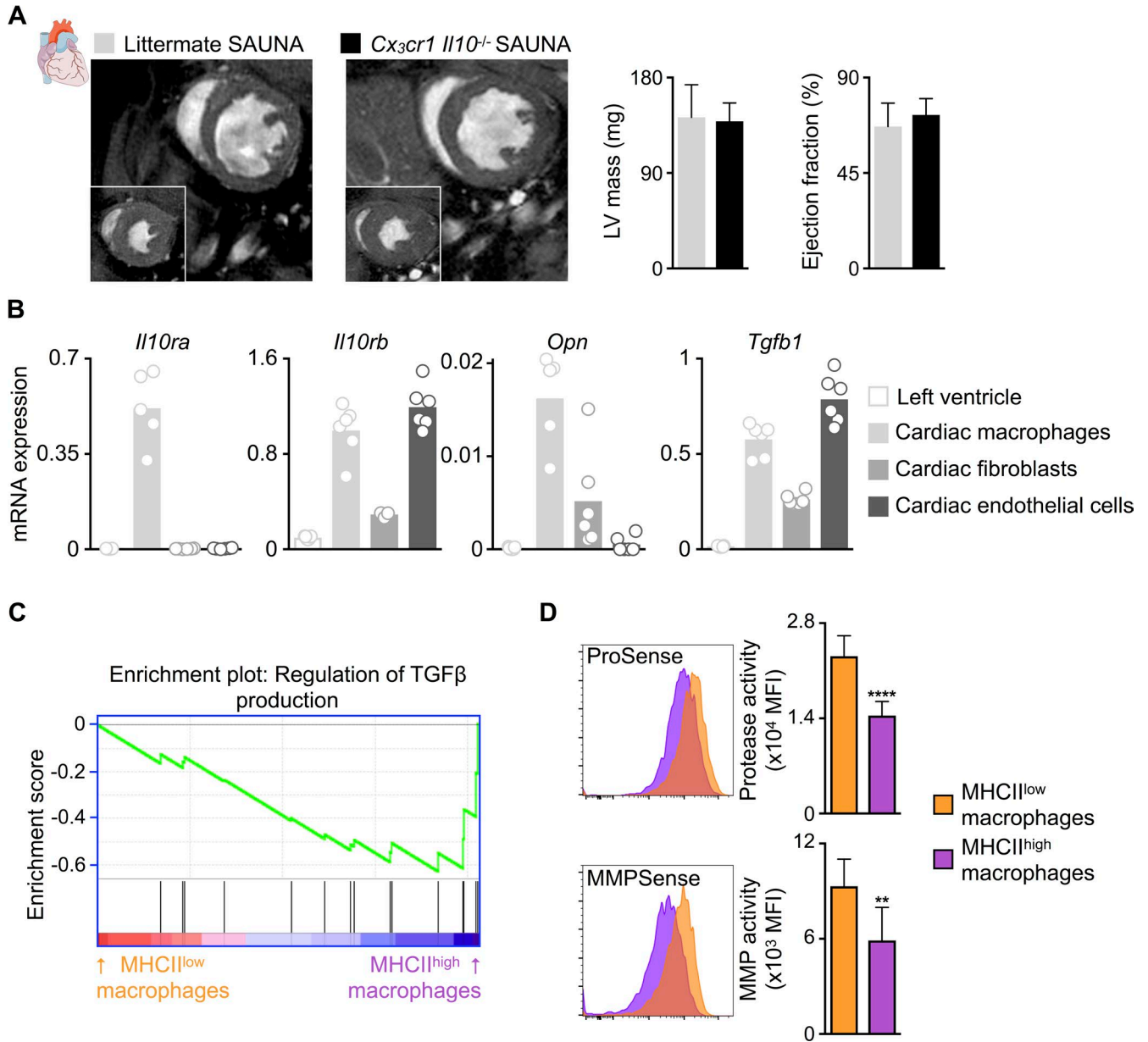


Figure S3. **Macrophage-restricted IL-10 deletion does not alter SAUNA-induced hypertrophy.** (A) Evaluation of LV mass and ejection fraction by cardiac magnetic resonance imaging in littermate and *Cx₃cr1* *Il10*^{-/-} SAUNA-exposed mice ($n = 5-10$ mice per group). Each panel shows the midventricular short-axis view at end diastole and end systole (inset). (B) Relative IL10 receptor (*Il10ra* and *Il10rb*), *Opn*, and *Tgfb1* expression levels by qPCR in left ventricle and FACS-purified cardiac macrophages, fibroblasts, and endothelial cells from C57BL/6 mice ($n = 5-9$ mice per group). The FACS-gating strategy used to purify macrophages, fibroblasts, and endothelial cells from heart tissue is shown in Fig. 7 D. (C) Gene set enrichment analysis of deposited microarray data (Epelman et al., 2014) shows that expression of genes involved in regulation of TGFβ production (GO:0032914) is higher in MHCII^{high} macrophages than in MHCII^{low} macrophages ($P = 0.028$, FDR = 0.125). (D) MFI indicating ProSense and MMP activity in MHCII^{low} (orange) and MHCII^{high} (purple) cardiac macrophages from C57BL/6 mice. Data are pooled from two independent experiments ($n = 9$ mice per group). Results are shown as mean ± SD. For statistical analysis, a two-tailed unpaired *t* test was performed to compare two groups. **, $P < 0.01$; ****, $P < 0.0001$.

Table S1. Clinical characteristics of patients recruited for LV myocardial biopsies.

Parameter	Hypertension without HFpEF (n = 4)	Hypertension with HFpEF (n = 6)
Age (yr)	61 ± 6	64 ± 10
Body surface area (kg/m ²)	2.2 ± 0.4	2.4 ± 0.2
Systolic blood pressure (mmHg)	133 ± 10	135 ± 17
Diastolic blood pressure (mmHg)	71 ± 8	72 ± 12
LV end-diastolic volume index (ml/m ²)	61 ± 12	57 ± 10
LV wall thickness (cm)	1.2 ± 0.2	1.3 ± 0.5
LV mass index (g/m ²)	106 ± 16	114 ± 15
Relative wall thickness	0.45 ± 0.06	0.49 ± 0.10
LV ejection fraction (%)	67 ± 4	71 ± 10
Left atrial volume index (ml/m ²)	25 ± 4	35 ± 5*
Pulmonary capillary wedge pressure (mmHg)	11 ± 2	16 ± 2**
LV end-diastolic pressure (mmHg)	12 ± 2	19 ± 5*

Data are mean ± SD. Two-tailed unpaired *t* test: *, *P* < 0.05; **, *P* < 0.01.

REFERENCE

Epelman, S., K.J. Lavine, A.E. Beaudin, D.K. Sojka, J.A. Carrero, B. Calderon, T. Brija, E.L. Gautier, S. Ivanov, A.T. Satpathy, et al. 2014. Embryonic and adult-derived resident cardiac macrophages are maintained through distinct mechanisms at steady state and during inflammation. *Immunity*. 40:91–104. <https://doi.org/10.1016/j.immuni.2013.11.019>